Journal of Neuropathology and Experimental Neurology
Vol. 62, No. 3
March, 2003
pp. 292–303

Posthemorrhagic Ventricular Dilation in the Neonate: Development and Characterization of a Rat Model

SHOBHA S. CHERIAN, MRCP, MRCPCH, SETH LOVE, PHD, FRCP, FRCPATH, IAN A. SILVER, FRCVS, MA, HELEN J. PORTER, MD, FRCPATH, ANDREW G. L. WHITELAW, MD, FRCPCH, AND MARIANNE THORESEN, MD, PHD, FRCPCH

Abstract. Intraventricular hemorrhage is a common complication of prematurity. Posthemorrhagic ventricular dilation (PHVD) has a high rate of disability and no safe and effective treatment. Its pathogenesis is poorly understood, largely because of the lack of a satisfactory animal model. We have developed a model of neonatal PHVD in the rat. Seven-day-old (P7) Wistar rat pups were given 80-μl injections of citrated rat blood or artificial cerebrospinal fluid (CSF) into alternate lateral ventricles on P7 and P8. Intracranial pressure was monitored and increased briefly by over 8-fold. Some rats received further 10-μl intraventricular injections of India ink on P21. Animals were weighed daily and simple neurologic tests performed. On P21 (or P22 if India ink had been injected), the rats were perfusion-fixed and blocks processed for paraffin histology. Sixty-five percent of pups injected with blood and 50% injected with artificial CSF developed dilated lateral ventricles, with patchy loss of ependyma, marked astrocytic gliosis, and rarefaction of periventricular white matter. India ink injection revealed slow transit of CSF from the dilated lateral ventricles but eventual passage into the subarachnoid space. Pups that had received intraventricular injections but did not develop ventricular dilation nonetheless had lighter brains than littermate controls ($p < 0.001$). Body weights were not significantly different from controls. Hydrocephalic animals had reduced motor performance as assessed by a grip traction test ($p = 0.0002$). This model is well suited to studying the pathogenesis of PHVD.

Key Words: Hydrocephalus; Neonates; Posthemorrhagic ventricular dilation; Prematurity; Ventricular hemorrhage; White matter damage.

INTRODUCTION

Intraventricular hemorrhage (IVH) affects approximately 15% of all prematurely born infants (1). In those weighing less than 1,000 g at birth, large hemorrhages that distend the lateral ventricles, with or without accompanying periventricular hemorrhagic infarction, are found in 10% to 20% of cases (2–4). Over half develop posthemorrhagic ventricular dilation (PHVD) and 60% to 80% of those suffer from long-term neurologic disability (5–7). Moreover, advances in neonatal intensive care facilitating the survival of increasing numbers of very low birth-weight babies have contributed to a rise in the incidence of this condition. No satisfactory treatment exists.

The pathogenesis of PHVD following IVH is not well understood. The conventional explanation for the impaired reabsorption of cerebrospinal fluid (CSF) is that channels in the arachnoid villi that project into the cranial venous sinuses are initially obstructed by microthrombi and subsequently by obliterative arachnoiditis (8, 9). Obstruction at the level of the aqueduct and outflow foramina of the fourth ventricle has also been demonstrated (10, 11).

A contributing factor may be inefficient fibrinolysis in the CSF due to low levels of plasminogen and high levels of plasminogen activator inhibitor (12, 13). Through mechanisms that are still obscure, IVH also seems to upregulate fibroblast activity within the subarachnoid space and possibly even the brain parenchyma, impairing fluid drainage along perivascular spaces within the brain as well impeding passage of CSF through the subarachnoid space and arachnoid villi (14–17). Transforming growth factor-β (TGF-β), and possibly other growth factors such as fibroblast growth factor, may be key mediators of this process (18–22).

A major limitation to progress in our understanding and management of PHVD has been the absence of an animal model to study the pathogenesis and explore potential treatments. Although there are several animal models of both hydrocephalus (18, 20, 22–38) and intraventricular hemorrhage (39–46), none adequately reproduces the development of ventricular dilation following IVH in a premature infant. The present study was therefore undertaken to develop and characterize such a model.

MATERIALS AND METHODS

Animals

All experimental protocols were carried out under British Home Office license in accordance with UK guidelines. Lactating female Wistar rats with timed litters culled to 10 pups were obtained from the University of Bristol Medical School animal house. Ambient lighting was controlled to simulate a 12-hour day/12-hour night cycle, and the rats were given free

From the Division of Child Health (SSC, MT) and Department of Paediatric Pathology (HJP), St. Michael's Hospital, Bristol; Department of Neuropathology (SL), Institute of Clinical Neurosciences, Frenchay Hospital, Bristol; Department of Anatomy (IAS), School of Veterinary Science, Bristol; Division of Child Health (AGLW), Medical School Unit, Southmead Hospital, Bristol, United Kingdom.

Correspondence to: Professor Seth Love, Department of Neuropathology, Institute of Clinical Neurosciences, Frenchay Hospital, Bristol BS16 1LE, United Kingdom. E-mail: seth.love@bris.ac.uk

Grant support: Action Research grant SP3654.

access to food and water. Seven-day-old pups (P7) were divided into several groups (Table 1).

Group 1 comprised 97 pups (from 11 litters) that were used for a series of pilot studies to establish the optimal duration of injection and maximum volume of injected blood that could be tolerated.

Group 2 consisted of 27 pups (from 3 litters), some of which were used for physiological observations (intracranial pressure and rectal temperature), while others were given intraventricular injections of India ink to monitor the passage of CSF from the dilated lateral ventricles over a 24-h period. The pups in the 3 litters were randomly allocated to each of these parts of the study.

Group 3 was divided into 2 subgroups: 3a) 43 pups from 6 litters were given a single injection of blood simulating 1 episode of intraventricular hemorrhage on P7, and 3b) 126 animals from 16 litters were given 2 injections that mimicked 2 episodes of IVH on 2 consecutive days (P7 and P8). In both groups (3a and 3b), the injection at P7 was of citrated rat blood at room temperature into the left lateral ventricle, as described below. In group 3b, a further injection of citrated rat blood was made at P8 into the right lateral ventricle.

Each group of animals had 5 sets of littermate controls: 1) juvenile controls (rat pups that had no procedure performed on them and remained with their dams); 2) unanesthetized controls (pups that were separated from their dams for a period matching that of the experimental animals, were not anesthetized, and had no procedures performed); 3) anesthetized controls (pups that were separated from the dams, were anesthetized for a period matching that of experimental animals, and underwent the same initial operative procedure as the experimental animals but did not have a needle inserted into the lateral ventricles); 4) sham-injected controls (separated and anesthetized for a period matching that of the experimental groups, subjected to scalp retraction and insertion of a needle into the lateral ventricles, but not injected with any fluid); and 5) controls given artificial CSF injection (separated, anesthetized, subjected to scalp retraction and needle insertion, and given an injection of artificial CSF at room temperature into the lateral ventricles). The artificial CSF (Manor Park Pharmaceuticals, Bristol, UK) consisted of 5.0 mmol/l glucose, 148 mmol/l sodium, 4.02 mmol/l potassium, 1.22 mmol/l magnesium, 1.36 mmol/l calcium, 133.8 mmol/l chloride, 0.58 mmol/l phosphate, 1.22 mmol/l sulphate, and 22 mmol/l bicarbonate; pH was 7.3.

Group 4 comprised 1 litter of 9 rat pups that received a bilateral injection of citrated rat blood and were allowed to survive for 48 days.

Collection and Preparation of Blood

Fresh blood for injection was collected on the day of the experiment from the tail vein or by cardiac puncture of an adult rat of the same inbred strain. This avoided immunologic incompatibility. After collection, the blood was mixed with buffered sodium citrate (136 μl of 0.105 M buffered citrate per ml of blood, pH 5.5) at room temperature and centrifuged at 6,000 rpm for 10 min. Most of the supernatant plasma (80%) was discarded and the packed cells and buffy coat layer were gently resuspended in the remaining plasma, with the aim of simulating the relatively high hematocrit (0.4–0.6) of human premature

TABLE 1
Treatment Groups and Numbers of Animals

Groups	Juvenile controls	Unanesthetized controls	Anesthetized controls	Sham injection	Sham CSF injection	Single IVH	Bilateral IVH	Total
Group 1		7 (2M, 5F)	7 (4M, 3F)			83 (41M, 42F)		97 (47M, 50F)
Group 2				2 (1M, 1F)	9 (3M, 6F)	4 (2M, 2F)	12 (9M, 3F)	27 (15M, 12F)
Group 3a	5 (3M, 2F)	6 (2M, 4F)	6 (3M, 3F)	5 (2M, 3F)	7 (3M, 4F)	14 (5M, 9F)		43 (18M, 25F)
Group 3b	16 (10M, 6F)	10 (6M, 4F)	9 (4M, 5F)	15 (4M, 11F)	22 (11M, 11F)		54 (24M, 30F)	126 (59M, 67F)
Group 4							9 (5M, 4F)	9 (5M, 4F)

M = male; F = female.

infants. The mean hemoglobin concentration (±SD) of the injected blood in the single-injection protocol was 20.9 ± 0.8 g/100 ml (range 19.4–22.0 g/100 ml), and that in the double-injection protocol 22.4 ± 1.9 g/100 ml (range 17.5–25.1) on P7 and 22.3 ± 2.1 g/100 ml (range 17.0–24.9) on P8.

Anesthesia and Injection into Ventricles

On P7 the rat pups were weighed and placed on a warming pad. Anesthesia was induced by inhalation of a mixture of halothane (3%–3.5% for induction and 1%–1.5% for maintenance) and 2:1 nitrous oxide and oxygen. A small incision was made in the midline over the scalp and the skin and subcutaneous tissues were retracted. The animal was then placed on a styrofoam mold in a modified Baltimore stereotactic frame, stereotactic zero having been defined in relation to the midline position of the horizontal ear bars. The animal was positioned with the tooth bar immediately behind the position of the incisor teeth and the ear bars in the position of the external auditory meatuses. Special care was taken to push the ear bars together very carefully, only until the first slight resistance was felt. The head was centered using the calibration on the ear bars. A 27-gauge needle (OD 0.4 mm) was held in the head-holder micromanipulator and connected by thin medical grade polyethylene tubing to a 1-ml syringe containing the prepared blood and activated by a syringe driver. The needle was positioned 1.7 mm to the left and 3.8 mm rostral to stereotactic zero and then inserted to a depth of 3.5 mm below the level of the skull in order to penetrate the lateral ventricle (47). In pilot experiments, various volumes of prepared blood (10 μl–120 μl [80 μl in the majority of cases]) were injected over 10 min and the needle then withdrawn over 4 min. After the injection, the rats were removed from the frame, placed on the warming pad, and allowed to recover for 5 min in 30% oxygen. They were then returned to the dam. The duration of anesthesia and of separation from the dam was recorded. The rat pups were weighed on most days from P7 to P21. On the basis of the findings in the preliminary experiments (see below), an injection volume of 80 μl was used in all subsequent experiments.

Neurologic Examination

On P21, two neurologic tests were performed on a subset of 52 rats. Twenty-four were juvenile controls, 15 received a bilateral injection of sham CSF, and 13 received a bilateral injection of citrated rat blood. The tests were carried out at the same time of the day-night cycle and were performed in the same order for all rats. To assess postural reflexes and laterality (if any) of lesions, the rat was held by its tail above the table; normal rats extend both forelimbs to the table (score 0) and rats with focal cerebral lesions flex the contralateral forelimb (score 1) (48, 49). In a modified grip traction test, a plastic tube 0.6 cm in diameter was placed horizontally above the table and the length of time (to a maximum of 60 seconds) that the rat could hang from the tube by its forepaws was noted (48, 50).

Intracranial Pressure Monitoring

Intracranial pressure was recorded continuously in 20 rat pups by use of a microsensor strain gauge transducer (Codman and Shurtleff, Inc., Raynham, MA) before, during, and after the ventricular injection. The transducer was inserted through a burr hole to a depth of 3 mm into the cerebral hemisphere contralateral to the injection. The burr hole was sealed with bone wax. Care was taken not to introduce air into the cranial cavity.

Temperature Monitoring

Rectal temperature was monitored continuously in 12 pups by means of a 0.5-mm-diameter Harvard Physitemp probe (Physitemp, Clifton, NJ). Animals used for ICP and temperature monitoring were excluded from further analysis.

Histology

At P21, 14 days after the simulated IVH, the pups were given an overdose of phenobarbitone (20 mg/kg) and fixed by transcardiac perfusion with buffered 4% formaldehyde. The brains were weighed (before draining the ventricular fluid) and subdivided coronally into a standard set of blocks for paraffin embedding. Five-μm-thick sections were obtained 0.4 and 2 mm rostral to the bregma and stained with hematoxylin and eosin (H&E). Some blocks were also stained by Perls' method for iron and immunostained for glial fibrillary acidic protein (GFAP) (see below).

India Ink Injection

Seven pups that had developed hydrocephalus (as evidenced by head enlargement) were reanesthetized on P21, placed in the stereotactic frame, and given a 10-μl injection of India ink into the left lateral ventricle. Subsequently, they were deeply anesthetized and fixed by transcardiac perfusion with 4% formaldehyde at 1 h, 6 h, and 24 h after the injection. The cranium was decalcified by immersion for 4 days in 10% formic acid and processed intact to paraffin wax. The wax-embedded cranium with enclosed brain was subdivided into 3-mm coronal blocks that were sectioned at 5 μm and stained with H&E.

Immunohistochemistry

Paraffin sections cut at 5 μm were stained for GFAP with mouse monoclonal antibody (M0761, Dako, Ely, Cambridge, UK) at a dilution of 1:1,200 overnight at room temperature. The immunostaining was performed using Vectastain Elite kit (Vector Laboratories, Burlingame, CA) according to the manufacturer's instructions except for substitution of affinity-purified, rat-adsorbed, biotinylated anti-mouse IgG (BA2001, Vector Laboratories) for the biotinylated universal antibody in the kit in order to prevent nonspecific background staining. The immunostained sections were counterstained with hematoxylin, dehydrated, and mounted.

Morphometry

The coronal area of both lateral ventricles was measured in H&E-stained sections in 2 planes, 0.4 and 2 mm anterior to the bregma. The measurements were made with the help of Histometrix software (Kinetic Imaging, Wirral, UK) driving a Leica DM microscope. The areas of the left and right lateral ventricles in the 2 planes were summed to obtain a composite value termed ''ventricular area.''

Statistical Analysis

Data were analyzed using the software package Statview v5.01 (Adept Scientific, Letchworth, UK). Student *t*-tests and ANOVA were used for comparing parametric distributions and

TABLE 2
Body Weight at P7, P14, and P21

Treatment groups	Single Injection				Bilateral Injection			
	Number	P7 weight (g)	P14 weight (g)	P21 weight (g)	Number	P7 weight (g)	P14 weight (g)	P21 weight (g)
Juvenile controls	5	*11.6 ± 1.8	26.1 ± 4.8	39.7 ± 7.6	16	12.9 ± 1.7	29.1 ± 4.0	43.7 ± 4.8
Unanesthetized controls	6	11.5 ± 0.7	26.3 ± 3.2	39.9 ± 5.6	10	12.2 ± 3.1	26.9 ± 3.4	41.1 ± 5.2
Anesthetized controls	6	11.9 ± 0.9	26.3 ± 3.4	40.1 ± 5.2	9	11.9 ± 2.6	24.1 ± 5.8	36.8 ± 8.6
Sham injection	5	11.7 ± 2.2	23.6 ± 5.1	37.7 ± 5.6	14	11.7 ± 2.5	25.2 ± 4.3	38.9 ± 5.1
Sham CSF injection	7	12.6 ± 1.4	25.5 ± 3.9	39.6 ± 4.3	16	12.8 ± 2.4	27.6 ± 6.8	42.6 ± 9.7
IVH	13	12.7 ± 2.2	26.3 ± 4.1	40.4 ± 4.7	43	13.3 ± 2.2	26.9 ± 3.9	41.4 ± 7.3
Total	42	12.2 ± 1.7	25.8 ± 3.9	39.8 ± 5.1	108	12.8 ± 2.4	26.9 ± 4.7	41.2 ± 7.2

* All weights expressed as mean ± SD.

Mann Whitney and Kruskal Wallis tests for comparing nonparametric data. Descriptive statistics are presented as mean ± SD. If the results include one or more data sets that are skewed by outliers, median values and, where relevant, ranges are also given. As there was no sex-related difference in any of the parameters studied, the subdivision of data according to sex has not been presented in the Tables or analyses.

RESULTS

Preliminary Experiments

Of the 97 rat pups (group 1) used for the preliminary experiments, 83 were injected with gradually increasing volumes of donor rat blood (10–120 μl) and 14 served as controls. Ventricular area in controls and animals injected with 70 μl or less (n = 28) never exceeded 1 mm^2 and the mean ± 1SD was 0.4 ± 0.2 mm^2. By contrast, ventricular area was much more variable in pups that had received injections of 80 μl: it ranged from 0.07 to 3.2 mm^2 (n = 57) and exceeded 1 mm^2 in 9 pups. Higher volumes tended to result in retrograde leakage of blood around the needle tract and caused subdural effusions. Therefore, 80-μl injections were used in all subsequent experiments and a ventricular area of 1 mm^2 was set as the threshold for diagnosis of ventricular dilation.

Single 80-μl Injection

Of the 43 rat pups in group 2 that received a single intraventricular injection, 1 died within half an hour of the injection, giving an overall mortality of 2.33%. Table 2 shows the mean weights of the pups at P7, P14, and P21. There was no difference in weight at any time point among the 6 groups of animals or in the duration of anesthesia or of separation from the dam. The average gain in weight from P7 to P21 was 26.5 ± 3.6 g (median 24.9, range 25.9–28.5 g).

All of the control animals except those injected with sham CSF had a ventricular area <1 mm^2, the range being 0.3 to 0.9 mm^2 (Table 3). One of 7 animals injected with sham CSF (14.3%) and 4 of 13 animals injected with blood (30.8%) developed ventricular dilation (i.e. ventricular area >1 mm^2). One of the latter showed massive enlargement with a ventricular area of 21.7 mm^2, however, when this animal was removed from the analysis the median area was 2.4 mm^2 and the range 1.5 to 4.6 mm^2.

Bilateral 80-μl Injections

Of the 126 rat pups that received bilateral injections, 11 of those injected with blood, 6 with sham CSF, and 1 that underwent the sham injection died, yielding a mortality of 20.4%, 27.3%, and 6.7% in these respective subgroups. These 11 survived for a mean ± SD of 36.4 h ± 44.9 h (median 12.8, range 0.1–144).

There was no significant difference in the weights at P7, P14, and P21 (Table 2), the duration of anesthesia on P7 and P8, or the duration of separation among the different groups. The mean ± SD gain in weight was 28.4 ± 5.5 g (median 28.9, range 10–41.9). As in the single injection experiments, none of the control animals except those injected with sham CSF developed ventricular dilation, the ventricular area ranging from 0.1 to 0.8 mm^2. In contrast, 8 of 16 rat pups (50%) injected bilaterally with sham CSF and 28 of 43 (65.1%) injected with blood bilaterally had a ventricular area >1 mm^2. The ventricular area in the animals that did develop ventricular distension ranged from 11.9 to 70.5 mm^2 in those injected with sham CSF, and 1.2 to 56.1 mm^2 in those injected with blood (Table 3; Figs. 1, 2).

Group 4 were given bilateral injections of blood and allowed to survive until P48. Five of the 9 pups survived for the 7 weeks, and in these pups the ventricular area was 34.9 ± 21.6 mm^2 (median 37.9, range 0.9 to 60.9). An attempt was made to evaluate head size objectively by measuring interaural distance at P7, P14, and P21 in live as well as in dead rat pups at P21. However, this proved a less reliable predictor of ventricular dilation than did simple naked-eye examination (Fig. 3), which allowed identification of ventricular dilation in 65% of animals.

TABLE 3
Ventricular Area and Brain Weight after Single or Bilateral Injection of Blood

Treatment groups	Single Injection				Bilateral Injection			
	Number of pups	Ventricular area (mm^2) Mean ± SD	Ventricular area (mm^2) Median (range)	Brain weight (g) Mean ± SD	Number of pups	Ventricular area (mm^2) Mean ± SD	Ventricular area (mm^2) Median (range)	Brain weight Mean ± SD
Juvenile controls	5	0.5 ± 0.1	0.5 (0.3–0.6)	1.7 ± 0.1	16	0.5 ± 0.2	0.5 (0.1–0.8)	1.8 ± 0.1
Unanesthetized controls	6	0.5 ± 0.1	0.6 (0.5–0.6)	1.6 ± 0.1	10	0.4 ± 0.2	0.3 (0.2–0.8)	1.8 ± 0.2
Anesthetized controls	6	0.6 ± 0.2	0.5 (0.4–0.9)	1.7 ± 0.1	9	0.4 ± 0.2	0.4 (0.2–0.8)	1.7 ± 0.2
Sham injection	5	0.6 ± 0.1	0.6 (0.4–0.6)	1.7 ± 0.1	14	0.5 ± 0.2	0.5 (0.3–0.8)	1.7 ± 0.1
Sham CSF injection								
ventricular area <1 mm^2	6	0.6 ± 0.2	0.6 (0.4–0.8)	1.7 ± 0.1	8	0.6 ± 0.2	0.6 (0.4–0.9)	1.6 ± 0.2
ventricular area >1 mm^2	1	1.5		1.7	8	34.4 ± 25.7	19.7 (11.9–70.5)	1.9 ± 0.2
IVH								
ventricular area <1 mm^2	9	0.7 ± 0.1	0.7 (0.5–0.9)	1.7 ± 0.1	15	0.5 ± 0.2	0.5 (0.1–0.9)	1.7 ± 0.2
ventricular area >1 mm^2	4	7.7 ± 9.4	3.5 (2.3–21.7)	1.8 ± 0.2	28	17.3 ± 15.9	10.0 (1.2–56.1)	1.8 ± 0.3

Fig. 1. Graphical illustration of ventricular area measurements in the rat pups given bilateral 80-μl intraventricular injections of blood and in the control groups. Each triangle represents a single animal. The values are shown as $\log_{10}$(ventricular area in mm^2). The threshold for diagnosis of ventricular dilation was set at 1 mm^2, corresponding to a logarithmic value of zero (indicated by the horizontal line). This threshold was exceeded in 8 of 16 rat pups (50%) injected bilaterally with sham CSF and 28 of 43 (65.1%) injected with blood, but in none of the noninjected controls.

Brain Weight

The mean brain weight at P21 in both single and bilateral injection groups is shown in Table 3. The brain weight of animals that were injected bilaterally with either substance was significantly heavier in those that developed ventricular dilation than in those that did not ($p = 0.01$, Mann-Whitney test). The brain weight of bilaterally injected pups was not, however, heavier than that of littermate controls that had received no ventricular injections, although it should be noted that CSF was not drained before weighing. Animals that received bilateral injections of blood or artificial CSF but did not develop ventricular dilation had significantly lighter brains than did littermate controls ($p < 0.001$, Mann-Whitney test). There was no significant difference in brain weight among animals with or without ventricular dilation after a single injection of blood or CSF.

Intracranial Pressure

Mean baseline intracranial pressure, as measured with the parenchymal probe, was 1.5 ± 0.7 mmHg. The pressure increased to a peak of 17.2 ± 6.0 mmHg at 8.1 ± 2.9 min after initiation of the injection. Once the injection was complete and the needle removed from the brain, the pressure dropped to a mean of 3.1 ± 1.9 mmHg. There was no significant difference in the intracranial pressure (as indicated by the area under the pressure-time curve)

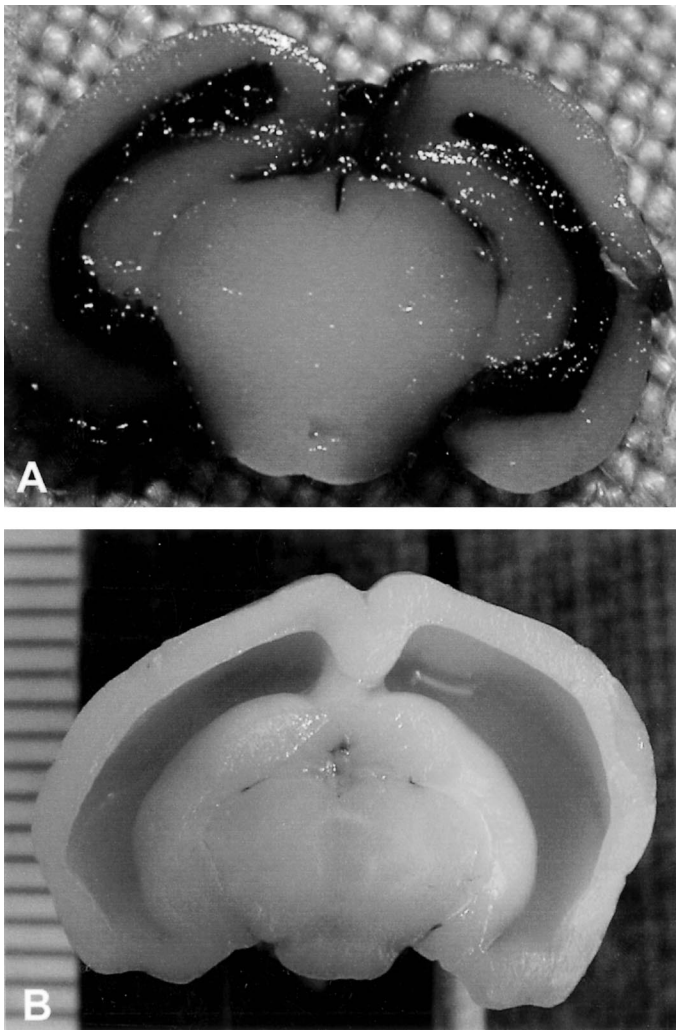

Fig. 2. Coronal brain slices through the cerebrum in a pup killed on P8 after the second injection of blood (**A**), and in a pup killed at P21 (**B**). The distension of the lateral ventricles by blood is clearly visible on P8. By P21 the ventricular blood has disappeared but the lateral ventricles are still dilated.

between the first and second injection of blood or artificial CSF or between injections of blood and those of CSF.

Temperature

The mean baseline temperature ± SD was 36.8 ± 1.5°C (median = 37.2). However, the rectal temperature dropped within 4 min to 34.8 ± 1.0°C (median = 34.7) once the pup was on the stereotactic frame. The temperature then stabilized and at the end of the injection it was 34.9 ± 0.9°C (median = 35.3).

Neurologic Assessment

Of the 52 rats tested, 8 of 15 injected on P7 and P8 with sham CSF, and 10 of 13 injected with blood developed ventricular dilation. In the postural reflex test all 52 rats showed no asymmetry in extension of their forelimbs.

Fig. 3. Enlargement of the head in association with PHVD. The P21 rat pup on the left received bilateral ventricular injections of blood on P7 and P8 and shows obvious doming of the head. Its littermate on the right was one of the normal juvenile controls.

When tested for grip traction there was a significant difference between the 3 groups ($p < 0.0005$, Kruskal Wallis test). There was no difference between juvenile controls and animals that did not develop ventricular dilation ($p = 0.12$, Mann-Whitney test). However, animals that did develop ventricular dilation were able to hang from the tubing for a significantly shorter time (22.3 ± 12.9 seconds, median = 18) than were those that did not (36.7 ± 10.5 seconds, median = 35; $p = 0.0002$, Mann-Whitney test).

Histology and Immunohistochemistry

Examination of rat pups from the noninjected control groups revealed no histologic abnormalities apart from occasional pyknotic neocortical and hippocampal neurons and focal disruption of cortex and white matter related to the insertion of a needle into the sham-injected controls. Examination of pups that had developed ventricular dilation showed most of the abnormalities to be related to the lateral ventricles and adjacent cerebral tissue. There was patchy loss of ependyma, astrocytic gliosis, and variable rarefaction of the periventricular white matter—in some cases associated with obvious edema (Fig. 4). Scattered hemosiderin-laden macrophages were present along the ventricular lining and in the adjacent white matter of rats that had been injected with blood. The strong Prussian blue staining of these macrophages when the sections were treated by Perls' method confirmed the nature of the pigment (Fig. 5). In many animals, both those injected with blood and those with CSF, it was possible to identify the injection track(s) as discrete linear regions of disruption of cortex and underlying white matter, with accumulation of lipid-laden macrophages and localized gliosis.

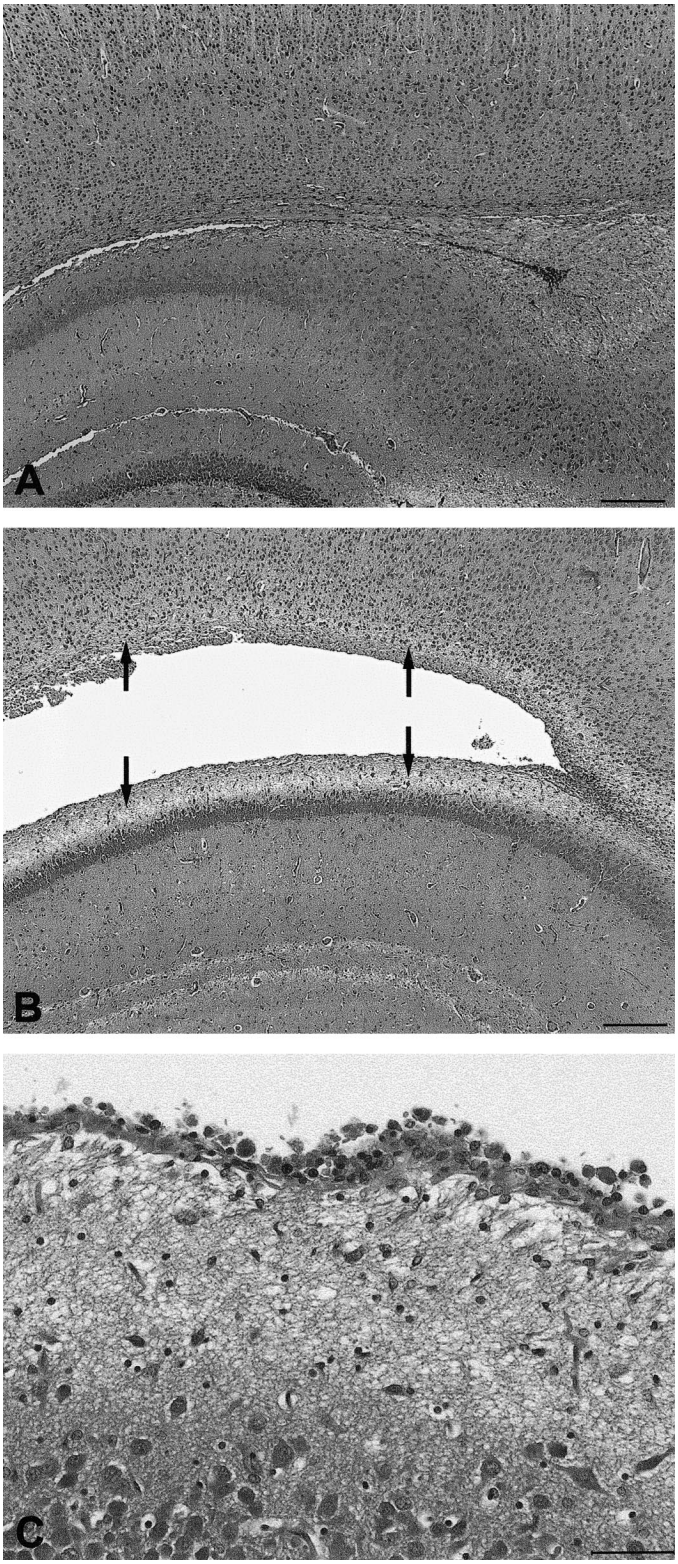

Fig. 4. Coronal sections at the same level through the lateral ventricle in a P21 animal with PHVD (**A**) and a normal littermate control (**B**). These figures are orientated with the hippocampus towards the bottom. The lateral ventricle is slit-like in the normal control but moderately enlarged in the animal with PHVD. Also visible in (**B**) is periventricular edema (arrows) and focal disruption of the ventricular lining (towards the left of the figure). **C**: At higher magnification, clusters of macrophages are visible adjacent to the ependyma and the periventricular tissue appears rarefied and gliotic. Scale bars: A, B = 250 μm; C = 20 μm. All sections stained with hematoxylin and eosin.

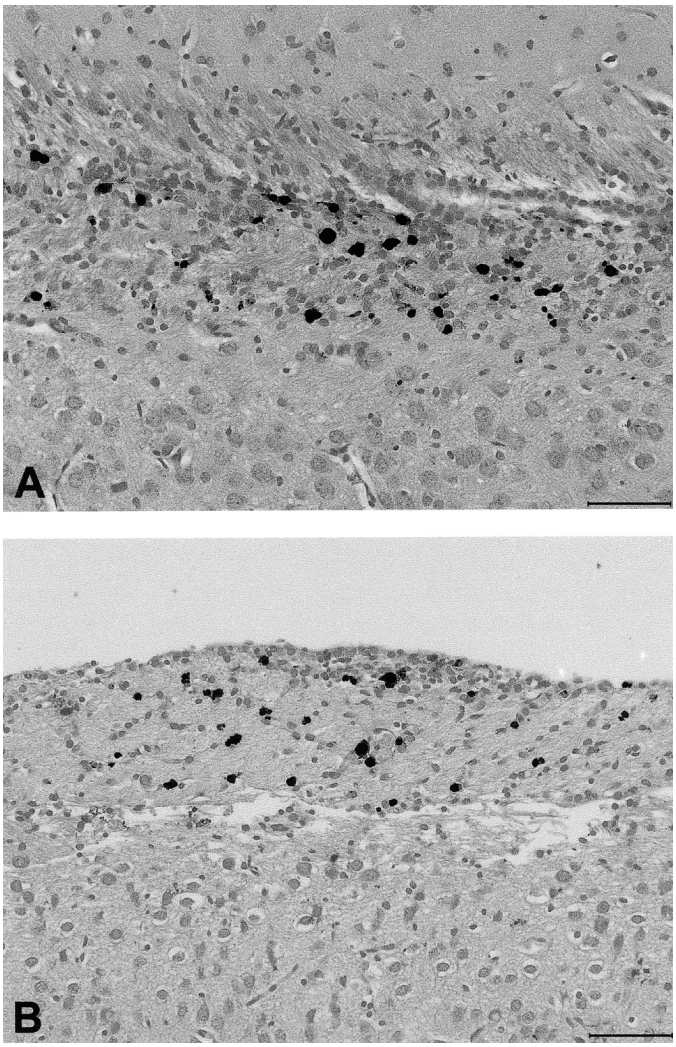

Fig. 5. Accumulation of hemosiderin pigment adjacent to lateral ventricles. Both (**A**) and (**B**) are sections of brain from rats given bilateral intraventricular injections of blood. Both sections contain hemosiderin-laden macrophages, although only 1 rat (**B**) developed PHVD. Hemosiderin was not seen after intraventricular injection of artificial CSF, even in rats that developed ventricular dilation. Scale bars = 40 μm. Perls' stain.

Apart from the disruption along the injection tracks and occasional pyknotic neocortical and hippocampal neurons, the cerebral gray matter in animals with ventricular dilation appeared largely intact. However, the region of hippocampus adjacent to the lateral ventricle contained increased numbers of astrocytes. Immunohistochemistry for GFAP revealed astrocytosis of the cerebral white matter and parts of the gray matter, especially

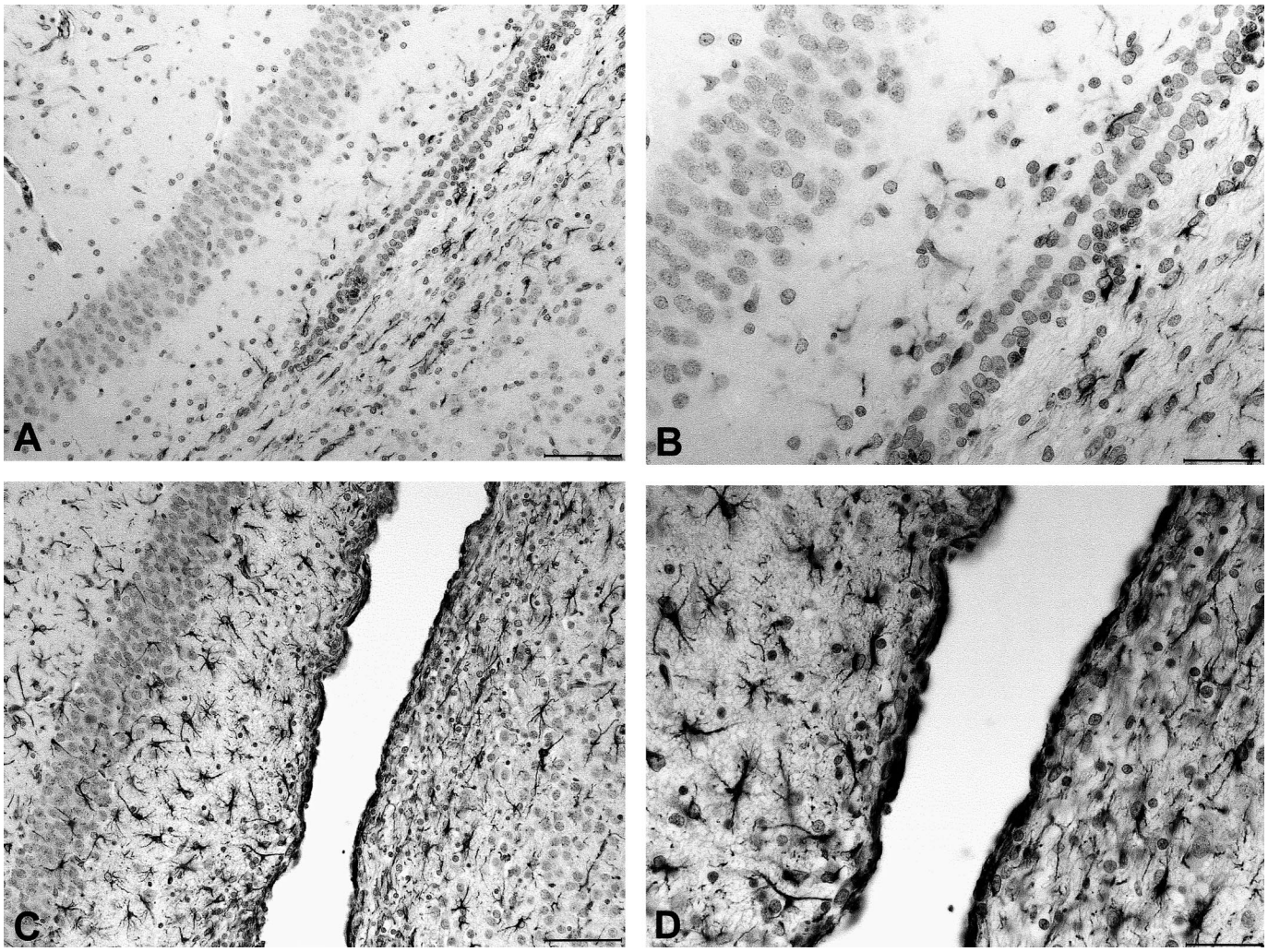

Fig. 6. Immunohistochemical demonstration of GFAP. **A**: Scattered immunolabeled astrocytes are present in a section of brain from a noninjected control rat. **B**: Higher magnification reveals labeled cells within the cerebral white matter and molecular layer of the hippocampus, but only scanty labeling immediately adjacent to the ependyma. **C**: In a rat with PHVD, labeled astrocytes are more numerous and more widely distributed, and their processes are more extensive. **D**: Higher magnification reveals a dense meshwork of GFAP-immunopositive processes along the lateral ventricle. Scale bars: A, C = 40 μm; B, D = 20 μm.

the regions of hippocampus abutting the lateral ventricle. A dense meshwork of subependymal GFAP-immunopositive processes was consistently present in the animals with ventricular dilation (Fig. 6). No consistent histologic differences were observed between animals with ventricular dilation due to injection of blood and those with dilation after injection of CSF.

Sections through the foramen of Munro, the third ventricle, aqueduct, and fourth ventricle showed these to be of normal caliber, with an intact ventricular lining and well-preserved adjacent brain tissue, even in animals with markedly dilated lateral ventricles. In a few animals there were clusters of macrophages in the foramen of Munro or the third ventricle but no other histologic abnormalities in these structures. No enlargement or other changes were seen in the subarachnoid space in relation to arachnoid villi or in the region of the cribriform plate.

In general, the rat pups that had received ventricular injections of CSF but did not develop dilation showed little in the way of histologic abnormalities other than those along the injection track and, in some cases, mild periventricular gliosis. In the animals that were injected with blood but did not show ventricular dilation at the time of histologic examination, scattered hemosiderin-laden macrophages were present in the deep white matter around the lateral ventricles, confirming that blood had been injected, despite the absence of subsequent ventricular dilation. The presence of the hemosiderin was confirmed using Perls' stain (Fig. 5). Hemosiderin was not present in sections of brain from rats that had been

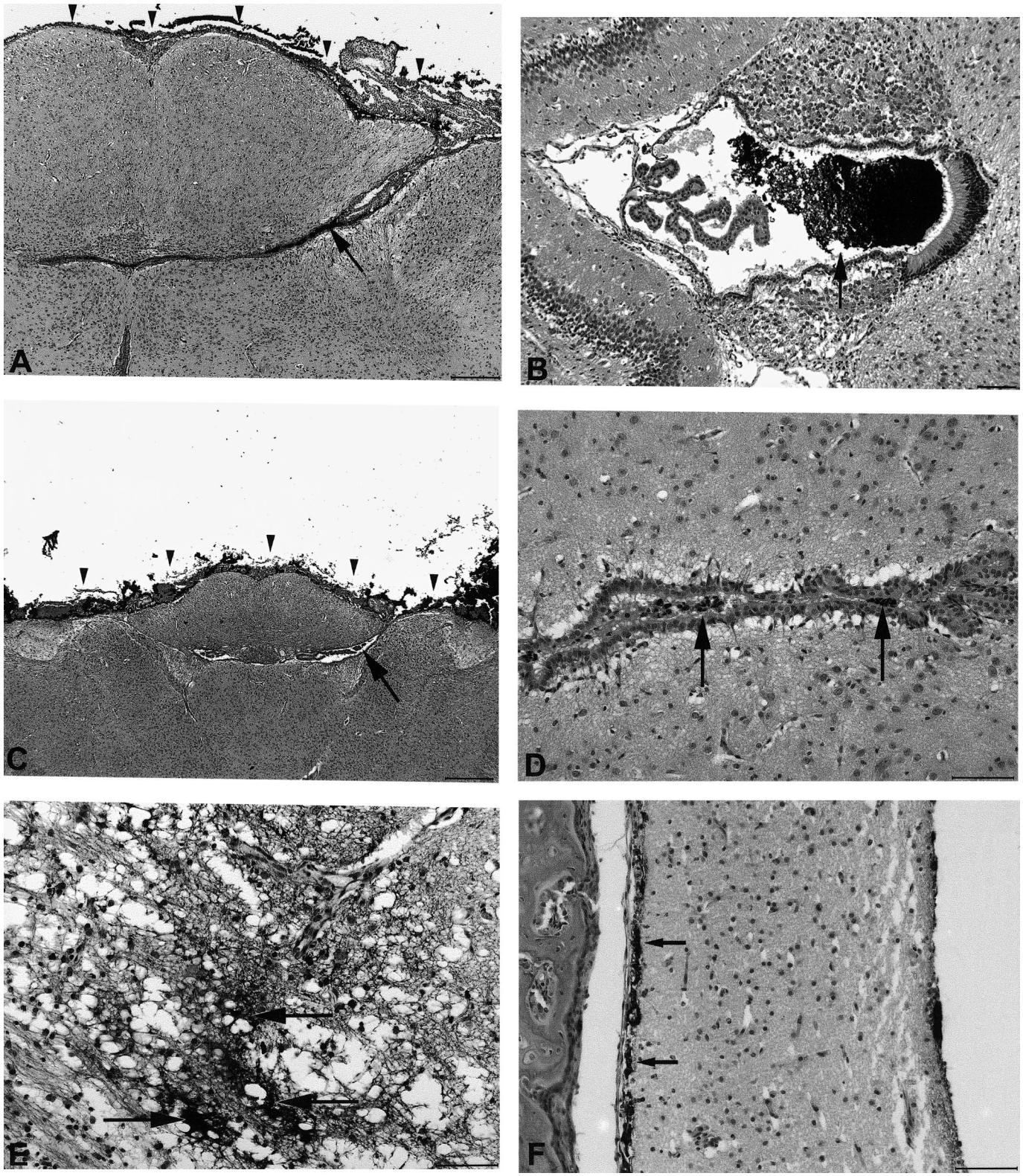

Fig. 7. India ink injection of dilated ventricles at P21. **A**: Section through the massively dilated lateral ventricles (towards top of figure) and deep gray matter in the plane of the foramen of Munro 1 h after injection of ink. Ink is present over the surface of the lateral ventricles (arrowheads), in the foramen of Munro (arrow), and in the anterior part of the third ventricle. Note that the foramen of Munro and anterior part of the third ventricle are of normal caliber. At 1 h, ink is also present in the body of the third ventricle (arrow) (**B**). At 24 h, ink still fills the dilated lateral ventricles (arrowheads) and foramen of Munro (arrow) (**C**) and a small amount of ink (arrows) is visible in the aqueduct (**D**). The deep cerebral white matter (**E**) contains accumulations of

injected with CSF, irrespective of whether or not these animals had developed ventricular dilation.

India Ink Study

Injected India ink was readily detected within the dilated lateral ventricles at 1 h and remained present in the lateral ventricles 6 h and 24 h after injection (Fig. 7). At all of these time points, and particularly at 24 h, scattered interstitial accumulations of India ink were present in the periventricular white matter around both lateral ventricles, indicating disruption of the ventricular lining and communication of fluid in the ventricle with the interstitial space in the deep white matter (Fig. 7e). At 1 h and 6 h, India ink could be seen in the third ventricle, and at 24 h ink was present in the subarachnoid space (Fig. 7f) and extending down the perivascular space of some of the cortical blood vessels. No ink was visible in the region of the cribriform plate or in nasal lymphatics.

DISCUSSION

We have developed an animal model of neonatal posthemorrhagic ventricular dilation, which to the best of our knowledge is the first such model reported. The model is easy to establish and mimics most of the pathologic features of posthemorrhagic hydrocephalus in the human neonate. As after ventricular hemorrhage in human neonates, ventricular dilation in this model is not inevitable but occurs in approximately 65% of rat pups injected with blood and 50% of those injected with artificial CSF. The development of hydrocephalus in a much higher proportion of rat pups given bilateral than unilateral injections of blood or CSF may reflect the situation in many premature infants that develop hydrocephalus after relatively protracted, often bilateral, ventricular hemorrhage. In addition, our rat pups with ventricular dilation showed reduced motor performance as revealed by the grip traction test. Over two-thirds of infants with progressive PHVD are known to develop motor deficits (5–7).

Early animal models of IVH relied on the development of spontaneous subependymal hemorrhages following premature delivery or after a variety of insults (e.g. hypotension or hypercarbia) in rabbit pups, preterm fetal sheep, and beagle pups (39–42). The hemorrhages that developed were similar to those seen in the newborn infant but ventricular dilation was not investigated, as survival was only short-term. Injection of blood mixed with thrombin into the lateral ventricles of adult pigs did not lead to posthemorrhagic ventricular dilation at 42-day follow-up (46). The only previous reports of PHVD in experimental studies were those of Pang et al (43–45), who stereotactically injected autologous clotted blood into the lateral ventricles of adult mongrel dogs. Eight of 10 dogs developed hydrocephalus 6 weeks later.

The adult rat has a hemoglobin concentration of 13 to 17 g/dl and a blood volume of 5.8 to 7.2 ml/100g body weight (51). The 80 μl of fluid that we injected to achieve ventricular dilation corresponds to approximately 12% of the circulating blood volume. Although this seems to be a large volume, it is not unusual to observe drops in hemoglobin of up to 50% in premature infants with large IVH. Because, in previous studies, injection of whole blood into the ventricles had not been reported to cause ventricular dilation (44–46), we used centrifuged blood, the cellular content of which was concentrated to the extent that hemoglobin content was elevated 1.5-fold. Our finding that injection of an equivalent volume of artificial CSF was as likely as blood to cause ventricular dilation that persisted to P21 was not expected. The absence of Perls'-positive material in the hydrocephalic animals that had been injected with artificial CSF excludes the possibility that the ventricular dilation was caused by bleeding due to the trauma of needle insertion. Our measurements showed intracranial pressure to increase to the same extent following the injection of either blood or CSF. This is not surprising because the rate of injection of 80 μl over 10 min exceeds by over 3-fold the rate of CSF production in an adult rat (22) and, therefore, substantially increases the volume of fluid in the ventricular system. Our findings suggest that acute ventricular distension and raised intracranial pressure are at least as important as the presence of blood and products of coagulation in the pathogenesis of chronic PHVD. These findings are consistent with the observation of Pang et al (44, 45) that in their adult canine model of ventricular hemorrhage, PHVD occurred only when there had been acute distension of the ventricles. Although we did not identify any consistent pathological abnormalities at the level of the foramen of Munro, the prolonged retention of India ink in the lateral ventricles suggests that there may have been a functional obstruction at this level. One possibility is that the roof of the interventricular foramen may have acted like a flap-valve, narrowing the foramen when pressure increased within the lateral ventricles.

Histologic observations and intracranial pressure measurements provide support for the concept that the initial ventricular dilation and increase in pressure can, and in many cases do, initiate a progressive pathologic process.

←

India ink (arrows) in the interstitial space. **F**: This section, taken 24 h after the injection of India ink, through meninges, part of the cerebral hemisphere, and a dilated lateral ventricle, shows some ink to have passed into the subarachnoid space (arrows). Scale bars: A = 125 μm; B = 50 μm; C = 250 μm; D, E, F = 40 μm.

Animals with hydrocephalus had much more severe gliosis, especially in the immediate subependymal region, than did those without hydrocephalus, despite having received ventricular injections of identical volume. However, the significantly lower brain weight in pups that did not develop hydrocephalus but had intraventricular injections of blood or artificial CSF indicates that the injections did have some adverse effect even in these animals. The consistent demonstration of hemosiderin-laden, Perls'-positive macrophages in the periventricular white matter after injection of blood is strong evidence that the pups were all correctly injected. It seems that the effects of the injection were related to processes within the brain only and not to any systemic complications, as the body:brain weight ratio was not different in any of the groups studied. Brain weights of animals with ventricular dilation were heavier than those without dilation because their ventricles were filled with CSF. In order to ensure good histologic preservation, the animals were fixed by transcardiac perfusion before the brains were removed and weighed, which may also have affected the brain weights, particularly in the hydrocephalic pups with white matter edema. Volumetric brain MRI studies have shown premature infants to have reduced cortical surface area and cortical gray matter volume at term gestation (52) and adolescence (53). Infants with periventricular leukomalacia also have reduced volumes of cortical gray and myelinated white matter (54). The present findings suggest that IVH may, even in the absence of PHVD, initiate pathologic processes that lead to a decrease in the volume of white and gray matter. Further investigations will be needed to elucidate the pathogenesis of the hydrocephalus and the loss of brain substance, whether or not the hydrocephalus and other abnormalities are progressive, and the reasons for the divergent reactions in different animals.

There are important differences between the development of the rat and that of the human brain. In humans, neuronogenesis is complete by 22 weeks, neuronal migration by 26 weeks, and glial cell proliferation peaks at 3 to 4 months of age (1, 55–57). In rats, however, neuronogenesis and migration peak just prior to birth (after gestation of 21 days) and continue for the first few days of life (58, 59). Glial cell proliferation in the rat is most intense at P1 to P20 (58). Synaptogenesis in man occurs predominantly between 2 months and 3 years of age, whereas myelination takes place from birth to several years postnatally (1). In the rat, synaptogenesis peaks at P14 to P21 and myelination at P10 to P50 (60–62). The rapid changes in development that occur in a rat brain from P7 to P21 are therefore different from those in human infants during the first few weeks of life. However, it should be noted that approximately 40% of adults who suffer a large IVH develop hydrocephalus (63), suggesting that maturity of the CNS may not be a key factor in development of PHVD. Our model may not be suitable for the study of all physiological and developmental consequences of PHVD. However, it is well suited to the examination of the cellular processes involved in the pathogenesis of this disabling condition, and to investigate possible interventions aimed at its prevention or amelioration.

REFERENCES

1. Volpe JJ. Neurology of the newborn. 4th Edition. Philadelphia: WB Saunders, 2000:428–93
2. Vohr BR, Wright LL, Dusick AM, et al. Neurodevelopmental and functional outcomes of extremely low birth weight infants in the National Institute of Child Health and Human Development Neonatal Research Network, 1993–1994. Pediatrics 2000;105:1216–26
3. Sheth RD. Trends in incidence and severity of intraventricular hemorrhage. J Child Neurol 1998;13:261–64
4. Synnes AR, Ling EW, Whitfield MF, et al. Perinatal outcomes of a large cohort of extremely low gestational age infants (twenty-three to twenty-eight completed weeks of gestation). J Pediatr 1994;125: 952–60
5. Ventriculomegaly Trial Group. Randomised trial of early tapping in neonatal posthaemorrhagic ventricular dilatation. Arch Dis Child 1990;65:3–10
6. International PHVD Drug Trial Group. International randomised controlled trial of acetazolamide and furosemide in posthaemorrhagic ventricular dilatation in infancy. Lancet 1998;352:433–40
7. Kennedy CR, Ayers S, Campbell MJ, et al. Randomized, controlled trial of acetazolamide and furosemide in posthemorrhagic ventricular dilation in infancy: Follow-up at 1 year. Pediatrics 2001;108: 597–607
8. Whitelaw A. Intraventricular haemorrhage and posthaemorrhagic hydrocephalus: Pathogenesis, prevention and future interventions. Semin Neonatol 2001;6:135–46
9. Whitelaw A, Thoresen M, Pople I. Posthaemorrhagic ventricular dilatation. Arch Dis Child Fetal Neonatal Ed 2002;86:F72–74
10. Larroche JC. Post-hemmorhagic hydrocephalus in infancy: Anatomical study. Biol Neonate 1972;20:287–99
11. Rorke LB. Pathology of perinatal brain injury. New York: Raven Press, 1972
12. Whitelaw A, Mowinckel MC, Abildgaard U. Low levels of plasminogen in cerebrospinal fluid after intraventricular haemorrhage: A limiting factor for clot lysis? Acta Paediatr 1995;84:933–36
13. Hansen A, Whitelaw A, Lapp C, Brugnara C. Cerebrospinal fluid plasminogen activator inhibitor-1: A prognostic factor in posthaemorrhagic hydrocephalus. Acta Paediatr 1997;86:995–98
14. McComb JG. Recent research into the nature of cerebrospinal fluid formation and absorption. J Neurosurg 1983;59:369–83
15. Sajanti J, Bjorkstrand AS, Finnila S, et al. Increase of collagen synthesis and deposition in the arachnoid and the dura following subarachnoid hemorrhage in the rat. Biochim Biophys Acta 1999; 1454:209–16
16. Sajanti J, Majamaa K. Detection of meningeal fibrosis after subarachnoid haemorrhage by assaying procollagen propeptides in cerebrospinal fluid. J Neurol Neurosurg Psychiatry 1999;67:185–88
17. Heep A, Stoffel-Wagner B, Soditt V, et al. Procollagen I C-propeptide in the cerebrospinal fluid of neonates with posthaemorrhagic hydrocephalus. Arch Dis Child Fetal Neonatal Ed 2002;87:F34–36
18. Galbreath E, Kim SJ, Park K, Brenner M, Messing A. Overexpression of TGF-beta 1 in the central nervous system of transgenic mice results in hydrocephalus. J Neuropathol Exp Neurol 1995;54:339–49
19. Kitazawa K, Tada T. Elevation of transforming growth factor-beta 1 level in cerebrospinal fluid of patients with communicating hydrocephalus after subarachnoid hemorrhage. Stroke 1994;25:1400–1404

20. Tada T, Kanaji M, Kobayashi S. Induction of communicating hydrocephalus in mice by intrathecal injection of human recombinant transforming growth factor-beta 1. J Neuroimmunol 1994; 50:153–58
21. Singer AJ, Clark RA. Cutaneous wound healing. N Engl J Med 1999;341:738–46
22. Johanson CE, Szmydynger-Chodobska J, Chodobski A, et al. Altered formation and bulk absorption of cerebrospinal fluid in FGF-2-induced hydrocephalus. Am J Physiol 1999;277:R263–71
23. Cohen AR, Leifer DW, Zechel M, et al. Characterization of a model of hydrocephalus in transgenic mice. J Neurosurg 1999;91:978–88
24. Shapiro K, Takei F, Fried A, Kohn I. Experimental feline hydrocephalus. The role of biomechanical changes in ventricular enlargement in cats. J Neurosurg 1985;63:82–87
25. Hochwald GM, Lux WE, Jr, Sahar A, Ransohoff J. Experimental hydrocephalus. Changes in cerebrospinal fluid dynamics as a function of time. Arch Neurol 1972;26:120–29
26. McAllister JP, Cohen MI, O'Mara KA, Johnson MH. Progression of experimental infantile hydrocephalus and effects of ventriculoperitoneal shunts: An analysis correlating magnetic resonance imaging with gross morphology. Neurosurgery 1991;29:329–40
27. Lovely TJ, McAllister JP, Miller DW, Lamperti AA, Wolfson BJ. Effects of hydrocephalus and surgical decompression on cortical norepinephrine levels in neonatal cats. Neurosurgery 1989;24: 43–52
28. Chumas PD, Drake JM, Del Bigio MR, Da Silva M, Tuor UI. Anaerobic glycolysis preceding white-matter destruction in experimental neonatal hydrocephalus. J Neurosurg 1994;80:491–501
29. Cosan TE, Gucuyener D, Dundar E, et al. Cerebral blood flow alterations in progressive communicating hydrocephalus: Transcranial Doppler ultrasonography assessment in an experimental model. J Neurosurg 2001;94:265–69
30. Ishizaki R, Tashiro Y, Inomoto T, Hashimoto N. Acute and subacute hydrocephalus in a rat neonatal model: Correlation with functional injury of neurotransmitter systems. Pediatr Neurosurg 2000;33: 298–305
31. Del Bigio MR, Vriend JP. Monoamine neurotransmitters and amino acids in the cerebrum and striatum of immature rats with kaolin-induced hydrocephalus. Brain Res 1998;798:119–26
32. Johnson RT, Johnson KP. Hydrocephalus as a sequela of experimental myxovirus infections. Exp Mol Pathol 1969;10:68–80
33. Johnson RT, Johnson KP. Hydrocephalus following viral infection: The pathology of aqueductal stenosis developing after experimental mumps virus infection. J Neuropathol Exp Neurol 1968;27:591–606
34. Margolis G, Kilham L. Induction of congenital hydrocephalus in hamsters with parainfluenza type 2 virus. Exp Mol Pathol 1977;27: 235–48
35. Jones HC, Bucknall RM. Inherited prenatal hydrocephalus in the H-Tx rat: A morphological study. Neuropathol Appl Neurobiol 1988;14:263–74
36. Jones HC, Harris NG, Briggs RW, Williams SC. Shunt treatment at two postnatal ages in hydrocephalic H-Tx rats quantified using MR imaging. Exp Neurol 1995;133:144–52
37. Jones HC, Richards HK, Bucknall RM, Pickard JD. Local cerebral blood flow in rats with congenital hydrocephalus. J Cereb Blood Flow Metab 1993;13:531–34
38. Tinsley CJ, Bennett GW, Mayhew TM, Parker TL. Stereological analysis of regional brain volumes and neuron numbers in rats displaying a spontaneous hydrocephalic condition. Exp Neurol 2001; 168:88–95
39. Lorenzo AV, Welch K, Conner S. Spontaneous germinal matrix and intraventricular hemorrhage in prematurely born rabbits. J Neurosurg 1982;56:404–10
40. Reynolds ML, Evans CA, Reynolds EO, et al. Intracranial haemorrhage in the preterm sheep fetus. Early Hum Dev 1979;3:163–86
41. Goddard J, Lewis RM, Alcala H, Zeller RS. Intraventricular hemorrhage—An animal model. Biol Neonate 1980;37:39–52
42. Ment LR, Stewart WB, Duncan CC, Lambrecht R. Beagle puppy model of intraventricular hemorrhage. J Neurosurg 1982;57: 219–23
43. Pang D, Sclabassi RJ, Horton JA. Lysis of intraventricular blood clot with urokinase in a canine model: Part 3. Effects of intraventricular urokinase on clot lysis and posthemorrhagic hydrocephalus. Neurosurgery 1986;19:553–72
44. Pang D, Sclabassi RJ, Horton JA. Lysis of intraventricular blood clot with urokinase in a canine model: Part 2. In vivo safety study of intraventricular urokinase. Neurosurgery 1986;19:547–52
45. Pang D, Sclabassi RJ, Horton JA. Lysis of intraventricular blood clot with urokinase in a canine model: Part 1. Canine intraventricular blood cast model. Neurosurgery 1986;19:540–46
46. Mayfrank L, Kissler J, Raoofi R, et al. Ventricular dilatation in experimental intraventricular hemorrhage in pigs. Characterization of cerebrospinal fluid dynamics and the effects of fibrinolytic treatment. Stroke 1997;28:141–48
47. Sherwood NM, Timiras PS. A sterotaxic atlas of the developing rat brain. Berkeley, CA: University of California Press, 1970
48. Bona E, Johansson BB, Hagberg H. Sensorimotor function and neuropathology five to six weeks after hypoxia-ischemia in seven-day-old rats. Pediatr Res 1997;42:678–83
49. Bederson JB, Pitts LH, Tsuji M, et al. Rat middle cerebral artery occlusion: Evaluation of the model and development of a neurologic examination. Stroke 1986;17:472–76
50. Combs DJ, D'Alecy LG. Motor performance in rats exposed to severe forebrain ischemia: Effect of fasting and 1,3-butanediol. Stroke 1987;18:503–11
51. Bivin SH, Crawford P, Brewer NR. The laboratory rat. Vol. 1, 1st Ed, 1979
52. Ajayi-Obe M, Saeed N, Cowan FM, Rutherford MA, Edwards AD. Reduced development of cerebral cortex in extremely preterm infants. Lancet 2000;356:1162–63
53. Nosarti C, Al Asady MH, Frangou S, et al. Adolescents who were born very preterm have decreased brain volumes. Brain 2002;125: 1616–23
54. Inder TE, Huppi PS, Warfield S, et al. Periventricular white matter injury in the premature infant is followed by reduced cerebral cortical gray matter volume at term. Ann Neurol 1999;46:755–60
55. Dobbing J, Sands J. Timing of neuroblast multiplication in developing human brain. Nature 1970;226:639–40
56. Dobbing J, Sands J. Quantitative growth and development of human brain. Arch Dis Child 1973;48:757–67
57. Mrzljak L, Uylings HB, Van Eden CG, Judas M. Neuronal development in human prefrontal cortex in prenatal and postnatal stages. Prog Brain Res 1990;85:185–222
58. Van Eden CG, Kros JM, Uylings HB. The development of the rat prefrontal cortex. Its size and development of connections with thalamus, spinal cord and other cortical areas. Prog Brain Res 1990; 85:169–83
59. Eayrs JT, Goodhead B. Postnatal development of the cerebral cortex in the rat. J Anatomy 1959;93:385–402
60. Bass NH, Netsky MG, Young E. Effects of neonatal malnutrition on developing cerebrum. I. Microchemical and histologic study of cellular differentiation in the rat. Arch Neurol 1970;23:289–302
61. Jacobson S. Sequence of myelination in the brain of the albino rat. Cerebral cortex, thalamus and related structures. J Comp Neurol 1963;121:5–29
62. Bass NH, Netsky MG, Young E. Effect of neonatal malnutrition on developing cerebrum. II. Microchemical and histologic study of myelin formation in the rat. Arch Neurol 1970;23:303–13
63. Goh KYC, Poon WS. Recombinant tissue plasminogen activator for treatment of spontaneous adult intraventricular hemorrhage. Surg Neurol 1998;50:526–32

Received September 16, 2002
Revision received October 30, 2002
Accepted November 12, 2002